



ELSEVIER

Thermochimica Acta 256 (1995) 325–338

thermochimica  
acta

## Thermal and reductive decomposition of ammonium thiomolybdates

Joaquín L. Brito \*, Marcel Ilija, Petra Hernández

*Laboratorio de Físicoquímica de Superficies, Centro de Química Instituto Venezolano de Investigaciones Científicas (I.V.I.C.) Apartado 21827, Caracas 1020-A, Venezuela*

Received 18 August 1994; accepted 25 October 1994

### Abstract

Thermal decomposition and hydrogen reduction of ammonium thiomolybdates of formulas:  $(\text{NH}_4)_2[\text{MoS}_4]$  (I),  $(\text{NH}_4)_2[\text{Mo}_2(\text{S}_2)_6] \cdot 2\text{H}_2\text{O}$  (II) and  $(\text{NH}_4)_2[\text{Mo}_3\text{S}(\text{S}_2)_6] \cdot 1.85\text{H}_2\text{O}$  (III), were investigated using thermogravimetric analysis (TGA), either in pure  $\text{N}_2$  or in 10%  $\text{H}_2$  in  $\text{N}_2$ , and temperature-programmed reduction (TPR). The thiomolybdate compounds were characterized by several physicochemical techniques, including FTIR, PAS/FTIR, UV-visible spectroscopy, XRD and CHNS elemental analyses. The decompositions of (I) and (II) proceed in a similar way independently of the type of gas phase, with production of  $\text{MoS}_3$ . However, the anion cluster of (III) is decomposed at lower temperatures in the presence of  $\text{H}_2$ . The amorphous  $\text{MoS}_3$  compound is very sensitive to the presence of  $\text{H}_2$ , which also lowers the onset of its decomposition. These results seem to support a model for the structure of  $\text{MoS}_3$ , consisting of triangular  $\text{Mo}_3$  cluster units, similar to those present in (III). TPR could be used as a “fingerprint” technique for identification of the complexes, as they present strong differences in the shapes and characteristic temperatures of the reductograms.

*Keywords:* Decomposition; Reducibility; Reductive decomposition; TGA; Thiomolybdate; TPR

### 1. Introduction

Thiomolybdate complexes and clusters have recently gained increased attention, due to their relevance to the bioinorganic chemistry of molybdenum [1] and as

\* Corresponding author.

models, or as precursors in novel synthetic routes, of sulfide-based hydroprocessing catalysts [2–5]. Molybdenum sulfides of technological interest, particularly  $\text{MoS}_2$  and  $\text{MoS}_3$ , can be prepared from thiomolybdate precursors.  $\text{MoS}_2$  is an important solid state lubricant and is thought to be one of the main active species in supported hydrodesulfurization (HDS) catalysts [6].  $\text{MoS}_3$  has been found to be promising as a cathode material for secondary ambient temperature alkali metal batteries [7].

In general, solid state characterization and reactivity data on these compounds is scarce. Although thermoanalytical techniques (TGA–DTG, DTA) have been employed to study the decomposition of some of the thiomolybdate complexes under inert gas atmospheres or vacuum [8,9], reports about their decomposition under reductive atmospheres are still lacking. In this regard, it must be noted that activation of heterogeneous catalysts often involves reductive pretreatments which generate active phases, e.g. metal particles, sulfides, carbides, nitrides, and even lower oxides which are not stable except under reaction conditions, from the air-stable, oxidic or passivated precursors. Temperature-programmed reduction (TPR) has been widely employed for the characterization of oxide-based catalysts [10,11], as well as other oxidic materials [12,13]. In principle, any reducible system can be explored by means of this technique. Nevertheless, there are few examples of its application to the characterization of sulfides or sulfided catalysts [14,15]. One reason for this state of affairs may be that catalytically active sulfides are quite difficult to handle after being generated, especially when well dispersed on catalytic supports, due to their very high sensitivity to ambient oxygen and moisture. In addition,  $\text{MoS}_2$  is known to be quite difficult to reduce [15].

The objective of this work was to study the decomposition under both inert and reductive atmospheres of the compounds  $(\text{NH}_4)_2[\text{MoS}_4]$ ,  $(\text{NH}_4)_2[\text{Mo}_2(\text{S}_2)_6] \cdot 2\text{H}_2\text{O}$  and  $(\text{NH}_4)_2[\text{Mo}_3\text{S}(\text{S}_2)_6] \cdot 1.85\text{H}_2\text{O}$ , employing thermal analysis techniques such as TGA and TPR. Recently it was reported that a pretreatment with  $\text{H}_2$  of the surface of  $\text{MoS}_2$  crystallites derived from the latter complex is *mandatory* to form active centers for the HDS of thiophene [2]. Hence, it is expected that the present results will prove to be of relevance in the characterization of molybdenum sulfide catalysts derived from these complexes.

## 2. Experimental

### 2.1. Preparation of the complexes

Ammonium tetrathiomolybdate,  $(\text{NH}_4)_2[\text{MoS}_4]$ , was synthesized using the method of Pan et al. [16]. The cluster compounds  $(\text{NH}_4)_2[\text{Mo}_2(\text{S}_2)_6] \cdot 2\text{H}_2\text{O}$  and  $(\text{NH}_4)_2[\text{Mo}_3\text{S}(\text{S}_2)_6] \cdot n\text{H}_2\text{O}$  were prepared according to the procedures reported as “method C” by Müller and Krickemeyer [17]. The complexes will be designated “monomer”, “dimer”, and “trimer”, respectively. Chemical reagents employed in the syntheses included: ammonium heptamolybdate (p.a., Merck), hydrogen sulfide (cp, Matheson), sulfur sublimed (Merck), and ammonium hydroxide (Lab. Grade, Fisher).

## 2.2. Physicochemical characterization of the complexes

UV-visible spectra of *N,N*-dimethylformamide solutions of the complexes were measured in a Spectronic 3000 Array spectrophotometer. FTIR spectra (as KBr pellets) were recorded on a Nicolet 5DXC instrument, which was also employed with an MTEC 200 attachment to obtain photoacoustic spectra (PAS/FTIR) of the pure undiluted samples. XRD powder traces were acquired with a Philips PW 1730 diffractometer, employing Co K $\alpha$ , Fe-filtered radiation. Elemental chemical analysis of H, N and S were performed with a Fisons 1800 CHNS-O Instrument.

## 2.3. Thermal analysis procedures

TGA experiments under dynamic inert atmosphere (N<sub>2</sub>, flowing at 100 ml min<sup>-1</sup>) were followed from room temperature to 1000°C at 10°C min<sup>-1</sup>, employing a Du Pont 951 Thermogravimetric Analyzer module connected to a 990 Thermal Analyzer console. As sulfur-containing samples can be oxidized at high temperature by residual air left in the Pyrex envelope of the control end of the balance, modifications to the glassware of the 951 analyzer as suggested by, for example, Chang and Jian [18] are recommended.

Some TGA runs were performed under an atmosphere of 10 vol% H<sub>2</sub> in N<sub>2</sub> (100 ml min<sup>-1</sup>), the remaining experimental conditions being the same as in the inert atmosphere experiments.

**WARNING:** Before admitting hydrogen, care has to be taken to evacuate the balance and/or flush the Pyrex envelope with pure inert gas (right hand side viewing from the front) in order to expel all the oxygen. It is important to realize that the control end of the balance houses electronic components and circuitry, which might ignite any H<sub>2</sub>/O<sub>2</sub> mixture.

TPR was performed in a Micromeritics TPD/TPR 2900 instrument. Samples ( $\approx$ 10 mg) were positioned on a quartz-wool plug in a U-tube quartz reactor. Measurements were carried out from room temperature to 1000°C at several heating rates (between 3 and 20°C min<sup>-1</sup>) under a 15 vol% H<sub>2</sub> in N<sub>2</sub> mixture. A liquid nitrogen trap before the thermal-conductivity detector allowed removal of all the H<sub>2</sub>O, H<sub>2</sub>S and NH<sub>3</sub> evolved during the measurements, the detector signal thus reflecting only the consumption of hydrogen. Quantification of the TPR spectra was performed employing CuO standards and the software for data acquisition and handling provided with the TPD/TPR 2900 by Micromeritics.

## 3. Results and discussion

### 3.1. Syntheses and characterization of the thiomolybdate complexes

The synthetic procedure reported by Pan et al. [16], which is an improvement on the method originally published by Kruss in 1884, resulted in the formation of

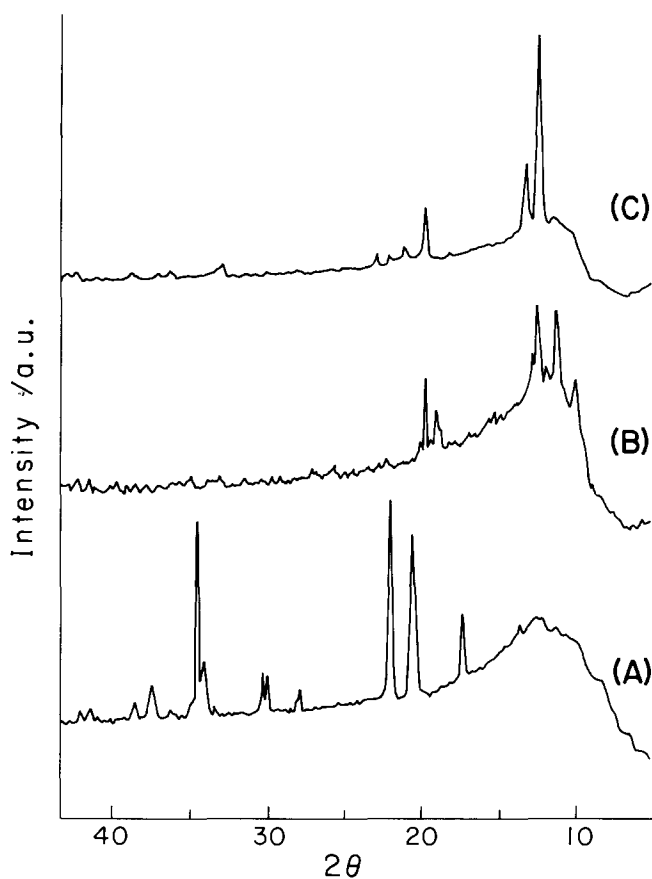


Fig. 1. X-ray powder diffractograms (Co  $K\alpha$ , Fe-filtered radiation) of (A)  $(\text{NH}_4)_2\text{MoS}_4$ ; (B)  $(\text{NH}_4)_2\text{Mo}_2\text{S}_{12} \cdot 2\text{H}_2\text{O}$ ; (C)  $(\text{NH}_4)_2\text{Mo}_3\text{S}_{13} \cdot 1.85\text{H}_2\text{O}$ .

highly crystalline monomer, in good yield ( $\approx 85\%$ ). The UV-VIS spectrum of this compound agrees with literature data [1a], showing no trace of  $(\text{NH}_4)_2[\text{MoOS}_3]$ , the main possible contamination of the monomer. The signal at  $476\text{ cm}^{-1}$  in the vibrational spectrum, observed by FTIR (at  $470\text{ cm}^{-1}$  by PAS) is characteristic of the  $\text{S}^{2-}$  ligands around the central  $\text{Mo}^{6+}$  core [19]. Chemical analyses results (H, 3.10%; N, 10.69%; S, 51.74%) closely match the theoretical calculations (H, 3.10%; N, 10.77%; S, 49.28%). The powder XRD trace is shown in Fig. 1, curve A. It must be noted that this trace is that of the well-ground material. The crystalline or insufficiently ground product showed strong variations in the intensities of several of the peaks, especially those at  $2\theta = 17.4$ ,  $22.1$ , and  $44.4^\circ$ , due to preferred orientation of the needle-shaped crystals [20]. Use of the crystals instead of the powder also brought other experimental problems during both TGA and XRD experiments, as explosive decomposition of the monomer crystals resulted in loss of

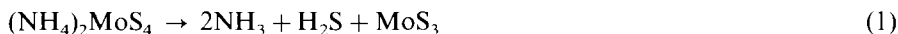
material from the sample pan or holder. Such problems were prevented by employing well-ground powder.

The dimer and trimer clusters were synthesized by method C of Müller and Krickemeyer [17]. The dimer is a black product, obtained in 26–30% yield. Its crystallinity degree varied strongly between different batches of similar preparations. The UV-vis spectrum is not very characteristic, as could be expected from its color; however, all the bands or shoulders previously reported [17] were identified. FTIR and PAS measurements showed the characteristic S–S stretching band at  $527\text{ cm}^{-1}$ . Elemental chemical analyses agree with the theory (H, 1.43% (1.86%); N, 4.08% (4.32%); S, 58.85% (59.31%)). The XRD powder pattern of a fairly crystalline sample is shown in Fig. 1, curve B.

The trimer was obtained as red crystals in 14–18% yield. It shows UV-VIS signals at 540 and 465 nm, and FTIR/PAS absorptions at 544, 512, 505 and  $459\text{ cm}^{-1}$ ; these measurements agree with published data [21]. Chemical analysis: H, 1.30%; N, 3.22%; S, 55.15%. Calculated for  $(\text{NH}_4)_2[\text{Mo}_3\text{S}(\text{S}_2)_6] \cdot 1.85\text{H}_2\text{O}$ : H, 1.52%; N, 3.62%; S, 53.85%. (The amount of hydration water was estimated from TGA experiments.) The XRD trace is shown in Fig. 1, curve C.

### 3.2. Thermal decomposition under inert atmosphere

Fig. 2 shows the simultaneous thermogravimetric (TG) and differential thermogravimetric (DTG) curves for the three complexes. Quantitative data derived from the TG curves is summarized in Table 1. The decomposition of the monomer (Fig. 2, curve A) has been studied by several workers, and is well understood (see, for example, Ref. [8] and references cited therein). Two TG regions can be seen, the first in the temperature region 120–260°C as a sharp step that corresponds to the loss of ammonia and hydrogen sulphide, according to the reaction



Molybdenum trisulphide thus generated decomposes in a broad temperature range (300–820°C) to  $\text{MoS}_2$ . Most of the corresponding weight loss occurs between 300 and 500°C, and the samples quenched at the latter temperature already show broad XRD features, characteristic of  $\text{MoS}_2$  (not shown). Kalthod and Weller [14] found that the Mo sulfide formed by heating samples of the monomer in He for 60 min at 450°C contained sulfur in excess of the  $\text{MoS}_2$  stoichiometry ( $\text{S}/\text{Mo} \approx 2.3$ ). Rode and Lebedev [22] reported that temperatures close to 800°C were necessary to attain an S/Mo ratio of 2.

To our best knowledge, the thermal decomposition of the dimer has not been reported in the literature, although the formation of gaseous  $\text{S}_2$  by decomposition at  $\approx 200^\circ\text{C}$  of the related  $\text{Cs}_2[\text{Mo}_2(\text{S}_2)_6]$  compound has been documented [23]. The dimer shows a more complex TGA pattern than the monomer (Fig. 2, curve B). The first two TG regions are poorly defined; at about 110°C there is a short plateau between two continuous weight loss regions, the weight at the plateau corresponding roughly to the evolution of two water molecules from the dimer. Weight loss up

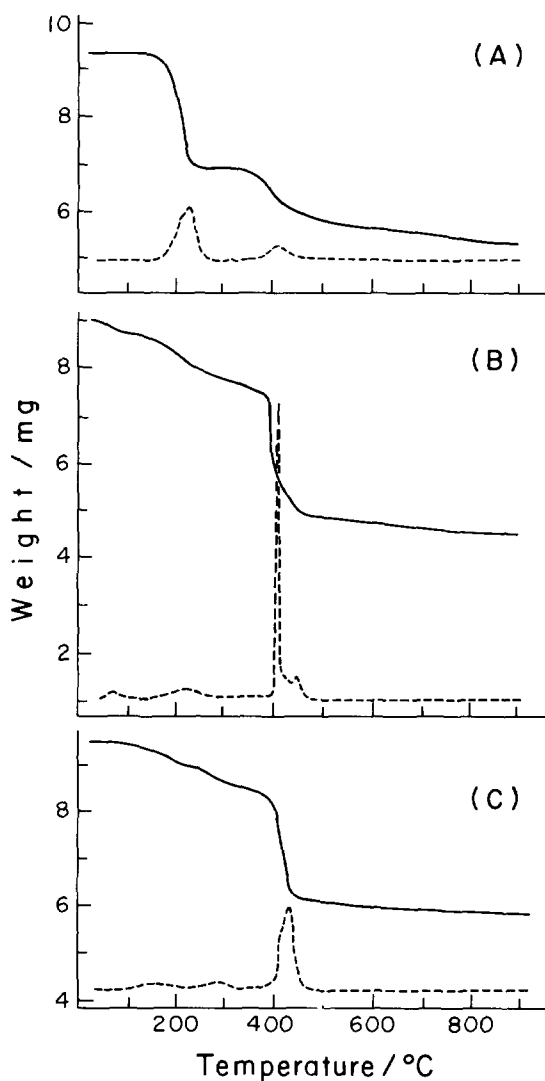
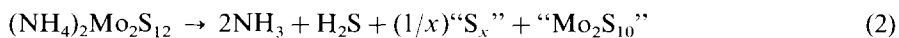


Fig. 2. Simultaneous TG (—) and DTG (---) curves at  $10^{\circ}\text{C}\ \text{in}^{-1}$  for the thermal decomposition in  $\text{N}_2$  atmosphere of (A)  $(\text{NH}_4)_2\text{MoS}_4$ ; (B)  $(\text{NH}_4)_2\text{Mo}_2\text{S}_{12} \cdot 2\text{H}_2\text{O}$ ; (C)  $(\text{NH}_4)_2\text{Mo}_3\text{S}_{13} \cdot 1.85\text{H}_2\text{O}$ .

to a solid product of composition “ $\text{Mo}_2\text{S}_{10}$ ” is observed in the region  $110\text{--}390^{\circ}\text{C}$ , suggesting evolution of ammonia, hydrogen sulfide and elemental sulfur



Between  $390$  and  $\approx 450^{\circ}\text{C}$  there is a very steep transition, but a definite change in slope can be observed at  $410^{\circ}\text{C}$ , where the observed weight suggests the formation of “ $\text{Mo}_2\text{S}_6$ ” or two mol  $\text{MoS}_3$  per mol of dimer. The region between  $410$  and  $800^{\circ}\text{C}$

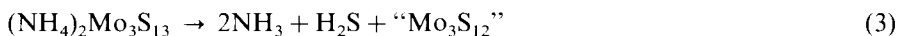
Table 1  
Thermal analysis data for decomposition of thiomolybdates in N<sub>2</sub> and in 10% H<sub>2</sub> in N<sub>2</sub>

Compound	Atmosphere	TG region	Temperature range/°C	Exerimental weight loss/%	Probable solid product	Calculated weight loss/%
(NH <sub>4</sub> ) <sub>2</sub> MoS <sub>4</sub>	N <sub>2</sub>	1	120–260	26.2	MoS <sub>3</sub>	26.18
		2	300–820	38.6	MoS <sub>2</sub>	38.50
(NH <sub>4</sub> ) <sub>2</sub> MoS <sub>4</sub>	H <sub>2</sub> /N <sub>2</sub>	1	110–240	25.9	MoS <sub>3</sub>	26.18
		2	240–400	38.8	MoS <sub>2</sub>	38.50
(NH <sub>4</sub> ) <sub>2</sub> Mo <sub>2</sub> S <sub>12</sub> · 2H <sub>2</sub> O	N <sub>2</sub>	1 <sup>a</sup>	r.t. 110	5.9	(NH <sub>4</sub> ) <sub>2</sub> Mo <sub>2</sub> S <sub>12</sub>	5.55
		2 <sup>a</sup>	110–390	19.0	“Mo <sub>2</sub> S <sub>10</sub> ”	21.00
		3	390–410	40.4	MoS <sub>3</sub>	40.77
		4	410–800	50.5	MoS <sub>2</sub>	50.65
(NH <sub>4</sub> ) <sub>2</sub> Mo <sub>2</sub> S <sub>12</sub> · 2H <sub>2</sub> O	H <sub>2</sub> /N <sub>2</sub>	1 <sup>a</sup>	r.t.–110	5.6	(NH <sub>4</sub> ) <sub>2</sub> Mo <sub>2</sub> S <sub>12</sub>	5.55
		2 <sup>a</sup>	110–385	20.6	“Mo <sub>2</sub> S <sub>10</sub> ”	21.00
		3	385–400	40.3	MoS <sub>3</sub>	40.77
		4	400–425	50.1	MoS <sub>2</sub>	50.65
(NH <sub>4</sub> ) <sub>2</sub> Mo <sub>3</sub> S <sub>13</sub> · 1.85H <sub>2</sub> O	N <sub>2</sub>	1 <sup>a</sup>	60–200	4.8	(NH <sub>4</sub> ) <sub>2</sub> Mo <sub>3</sub> S <sub>13</sub>	4.31
		2 <sup>a</sup>	210–400	12.2	“Mo <sub>3</sub> S <sub>12</sub> ”	13.11
		3	400–850	37.6	MoS <sub>2</sub>	37.96
(NH <sub>4</sub> ) <sub>2</sub> Mo <sub>3</sub> S <sub>13</sub> · 1.85H <sub>2</sub> O	H <sub>2</sub> /N <sub>2</sub>	1 <sup>a</sup>	80–210	4.2	(NH <sub>4</sub> ) <sub>2</sub> Mo <sub>3</sub> S <sub>13</sub>	4.31
		2 <sup>a</sup>	210–330	9.4	“Mo <sub>3</sub> S <sub>13</sub> ”	8.97
		3	330–440	38.5	MoS <sub>2</sub>	37.96

<sup>a</sup> Progressive weight loss (without clear DTG peaks).

corresponds to the decomposition of  $\text{MoS}_3$  to  $\text{MoS}_2 + x$ , with  $x$  initially decreasing quickly then gradually to zero.

The trimer also shows a somewhat complicated TGA trace. After dehydration, there is again a short plateau, this time at about  $210^\circ\text{C}$ , with a weight loss slightly larger than that corresponding to the evolution of  $1.85 \text{ mol H}_2\text{O/mol complex}$ . Between  $210$  and  $400^\circ\text{C}$  the weight loss roughly agrees with the reaction



The decomposition to  $\text{MoS}_2$  occurs as a single step starting at  $400^\circ\text{C}$ . As in the two former cases, the final product slowly but continuously loses weight up to  $850^\circ\text{C}$ . A previous report on the thermal decomposition of this cluster corresponds to TGA runs under vacuum [9a] which show a slightly different behavior, with lower temperatures for some of the regions and/or transitions (see next section).

These results show good agreement with the known reactivity in solution of the different types of sulfur ligands in these compounds [24]. The decomposition of the monomer, with only terminal sulfido groups, proceeds at lower temperatures than the release of the  $\mu_3\text{-S}^{2-}$  group in the trimer, whereas  $\text{S}_2^{2-}$  disulfido ligands in general evolve at higher temperatures than the sulfido ones.

### 3.3. Reductive decomposition under $\text{H}_2 + \text{N}_2$ mixture

TPR runs at  $10^\circ\text{C min}^{-1}$  are shown in Fig. 3. Numerical data derived from these experiments is displayed in Table 2. Qualitatively, it is interesting that the three complexes show strong differences in the peak shapes and characteristic temperatures ( $T_m$ , temperature at the maxima of the peaks). This result suggests that TPR could be employed as a fingerprint technique to detect the presence of the complexes or related structures, e.g. in supported catalysts. Spectra taken at other heating rates ( $\beta$ ) show similar features, although  $T_m$  varies with  $\beta$  (Table 3). This variation of  $T_m$  with  $\beta$  allows the calculation of the activation energy ( $E_a$ ) of the reduction by means of the model of Ozawa [25]. The values obtained for  $E_a$  as well as the correlation coefficients for the least-squares fitting of the  $\log \beta$  versus  $1/T_m$  plots are also shown in Table 3.

TPR spectra at  $10^\circ\text{C min}^{-1}$  (Fig. 3) show that the monomer is reduced at the lowest temperature ( $T_m$ ,  $260^\circ\text{C}$ ); the amount of hydrogen consumed corresponds to about  $1.3 \text{ mole H}_2 \text{ per mole of complex}$ . The dimer exhibits the highest  $T_m$  and also the sharpest TPR signal. The mole ratio  $\text{H}_2/\text{complex}$  is  $\approx 4.6$ . The trimer presents the broadest TPR signal, centered at  $340^\circ\text{C}$ . The amount of hydrogen consumed is approx.  $7.2 \text{ mole H}_2 \text{ per mole of complex}$ . The only previous report of TPR experiments on a similar material is that by Kalthod and Weller [14], regarding the reduction of  $\text{MoS}_3$  prepared by thermal decomposition of the monomer. These authors found two TPR peaks, at  $180$  and  $390^\circ\text{C}$ , using a heating rate of  $15^\circ\text{C min}^{-1}$ . However, it must be noted that their measurements involved the  $\text{H}_2\text{S}$  generated from the sample instead of the  $\text{H}_2$  consumed in the reaction. It is possible that the first TPR peak reflects  $\text{H}_2\text{S}$  retained in the material after the thermal decomposition of the monomer; it would desorb in a non-reductive process. In



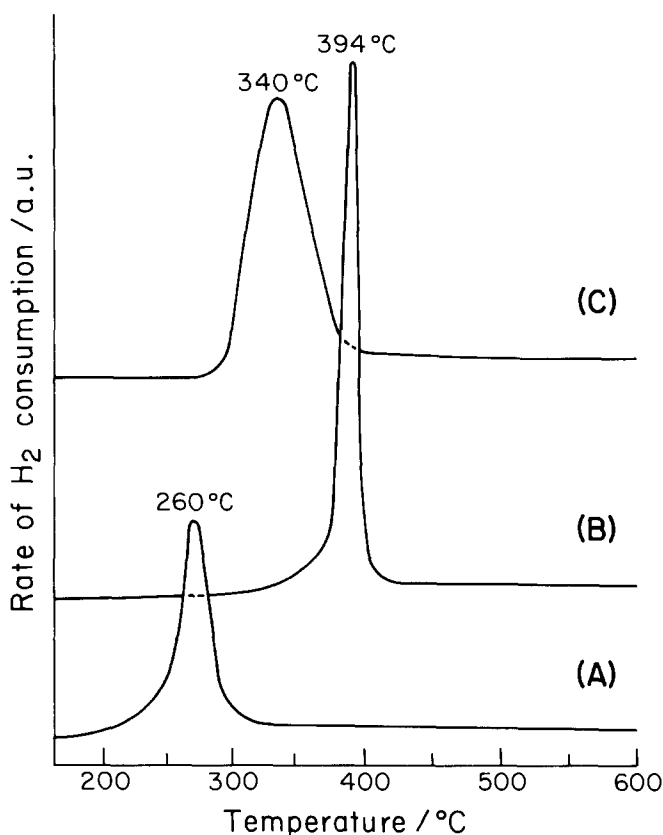


Fig. 3. Temperature-programmed reduction curves at  $10^{\circ}\text{C min}^{-1}$  of (A)  $(\text{NH}_4)_2\text{MoS}_4$ ; (B)  $(\text{NH}_4)_2\text{Mo}_2\text{S}_{12} \cdot 2\text{H}_2\text{O}$ ; (C)  $(\text{NH}_4)_2\text{Mo}_3\text{S}_{13} \cdot 1.85\text{H}_2\text{O}$ .

addition, their quantitative data show that, in general, less than 0.5 mol  $\text{H}_2\text{S/mol MoS}_3$  were detected during these experiments. This amount is significantly lower than the 1:1 ratio anticipated (see below).

TGA measurements for the monomer in  $\text{H}_2/\text{N}_2$  atmosphere (Fig. 4 and Table 1) show that the first decomposition step appears in a similar temperature range as in

Table 2  
Quantitative data calculated from the TPR spectra<sup>a</sup>

Compound	Amount of thiomolybdate/ $\mu\text{mol}$	Hydrogen consumption/ $\mu\text{mol H}_2$	$\text{H}_2$ :thiomolybdate mole ratio
$(\text{NH}_4)_2\text{MoS}_4$	$38 \pm 1$	$48 \pm 1$	$1.26 \pm 0.03$
$(\text{NH}_4)_2\text{Mo}_2\text{S}_{12} \cdot 2\text{H}_2\text{O}$	$15.4 \pm 0.4$	$71 \pm 2$	$4.6 \pm 0.1$
$(\text{NH}_4)_2\text{Mo}_3\text{S}_{13} \cdot 1.85\text{H}_2\text{O}$	$13.0 \pm 0.3$	$93 \pm 1$	$7.15 \pm 0.08$

<sup>a</sup> Heating rate  $\beta = 10^{\circ}\text{C min}^{-1}$ .

Table 3  
TPR peak maxima and activation energies of reduction of thiomolybdates

Compound	$T_m/^\circ\text{C}$					$E_a/(\text{kJ mol}^{-1})$	$r^b$
	$\beta = 3^a$	$\beta = 5$	$\beta = 10$	$\beta = 15$	$\beta = 20$		
$(\text{NH}_4)_2\text{MoS}_4$	220	235	260	281	300	$55 \pm 5$	0.989
$(\text{NH}_4)_2\text{Mo}_2\text{S}_{12} \cdot 2\text{H}_2\text{O}$	359	379	394	404	413	$165 \pm 15$	0.993
$(\text{NH}_4)_2\text{Mo}_3\text{S}_{13} \cdot 1.85\text{H}_2\text{O}$	292	312	340	360	376	$72 \pm 7$	0.999

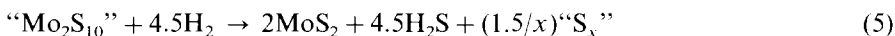
<sup>a</sup>  $\beta$  in  $^\circ\text{C min}^{-1}$ . <sup>b</sup> Correlation coefficients for the least-squares fitting of  $\log \beta$  vs.  $1/T_m$  (in K).

inert atmosphere, but the (reductive) decomposition of  $\text{MoS}_3$  to  $\text{MoS}_2$  starts at  $\approx 230^\circ\text{C}$ , in agreement with the TPR experiments. This temperature is about  $70^\circ\text{C}$  below that observed in pure  $\text{N}_2$ . In this case the plateau of the second TG region is reached at  $450^\circ\text{C}$ , the final weight corresponding to the reaction



According to the stoichiometry shown in reaction (4), the TPR results (Table 2) indicate that there is an excess of about 0.3 mol  $\text{H}_2/\text{mol}$  complex. At least part of this excess hydrogen is probably sorbed into the solid  $\text{MoS}_2$  generated, as has been previously found by several workers (see, for example, Komatsu and Hall [26] and references cited therein). The relatively large amount of hydrogen found in the present work may be accounted for by realizing that our  $\text{MoS}_2$  sample is generated at fairly low temperatures, and thus that its porosity and surface area should be large. Both these parameters have a considerable influence on the amount of sorbed  $\text{H}_2$  [26].

In the case of the dimer, the effect of hydrogen in the decomposition of the cluster anion is also minimal, as can be appreciated from the data in Table 1. The main difference between the TGA runs under  $\text{N}_2$  and under the  $\text{H}_2 + \text{N}_2$  mixture is that the final transformation of  $\text{MoS}_3$  to  $\text{MoS}_2$  is completed at  $425^\circ\text{C}$ , instead of the  $800^\circ\text{C}$  required under inert atmosphere. Other differences in the limiting temperatures of the TG regions are very small and within the experimental error of the measurements. Again, as in the case of pure inert atmosphere, there is a definite “break” in the TG (and DTG) curve for a composition corresponding to  $\text{MoS}_3$ . A comparison with the TPR data (Table 2) indicates that  $\approx 4.5$  mol  $\text{H}_2/\text{mol}$  complex are consumed in the TG regions 3 and 4. Hence, part of the decomposition occurs with evolution of elemental sulfur, probably formed by an intramolecular redox mechanism



The behavior shown by the trimer is different from those observed for the other two compounds, as  $\text{H}_2$  is actually involved in the decomposition of the complex. In the absence of  $\text{H}_2$ , the cluster decomposes gradually to “ $\text{Mo}_3\text{S}_{12}$ ” at  $400^\circ\text{C}$ , before the sharp transition to  $\text{MoS}_{2+x}$ . If hydrogen is present the cluster maintains its

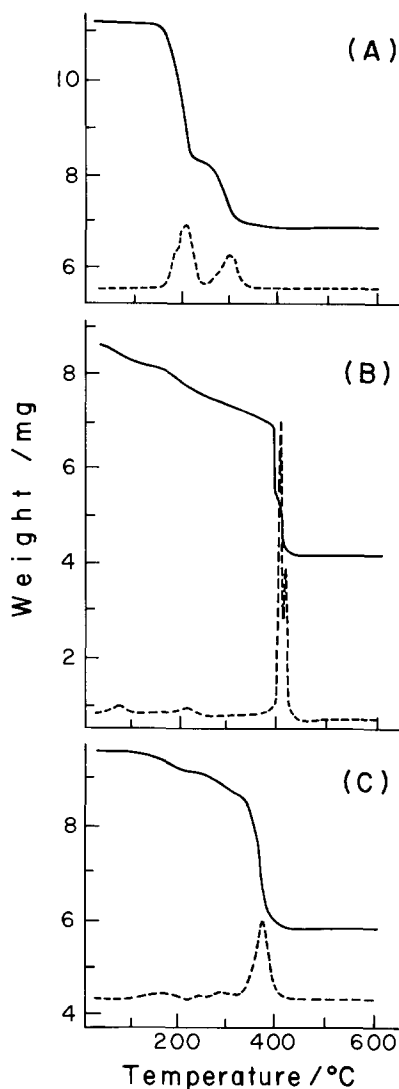


Fig. 4. Simultaneous TG (—) and DTG (---) curves at  $10^{\circ}\text{C min}^{-1}$  for the reductive decomposition in  $\text{H}_2 + \text{N}_2$  atmosphere of (A)  $(\text{NH}_4)_2\text{MoS}_4$ ; (B)  $(\text{NH}_4)_2\text{Mo}_2\text{S}_{12} \cdot 2\text{H}_2\text{O}$ ; (C)  $(\text{NH}_4)_2\text{Mo}_3\text{S}_{13} \cdot 1.85\text{H}_2\text{O}$ .

integrity up to  $330^{\circ}\text{C}$ , when decomposition to  $\text{MoS}_2$  starts and proceeds in a single stage; the  $\approx 7$  mol  $\text{H}_2$ /mol trimer consumption found by TPR confirms that gas-phase hydrogen is involved in the evolution of all the sulfur groups. In the other two cases, the first sulfur evolution proceeds identically in either atmosphere, without any gas-phase  $\text{H}_2$  involved. Curiously, the decomposition of the trimer under the  $\text{H}_2 + \text{N}_2$  mixture resembles that reported for the same compound under vacuum [9a], at least in the limits of the temperature regions.

It is interesting to note that  $\text{MoS}_3$  seems to be formed as an intermediate product in the thermal decomposition of both the monomer and the dimer, but not of the trimer. The presence of  $\text{H}_2$  in the reaction atmosphere has no influence in the formation of  $\text{MoS}_3$ , although the reactivity of this compound is much enhanced in  $\text{H}_2$  as compared to the inert atmosphere. The structure of the trisulphide, a non-crystalline solid, as well as the oxidation state of Mo in this material, have been subjects of controversy [27,28]. Earlier workers regarded  $\text{MoS}_3$  simply as an intimate mixture of  $\text{MoS}_2$  and amorphous sulfur [29]; however, Diemann [30] by means of X-ray radial distribution analysis, and Chang and Chan [19] employing FTIR and Raman, concluded that  $\text{MoS}_3$  is a distinct compound. Chien et al. [27] provided a chain model with  $\text{Mo}^{\text{V}}-\text{Mo}^{\text{V}}$  dimeric units, derived mainly from structural data and computer calculations. However, Müller et al. [28], on both chemical and structural grounds, favor a short-range-order model consisting of triangular Mo(IV) units, which, however, would not be the only constituents of this material.

During the decomposition of the trimer, formation of  $\text{MoS}_2$  from the discrete cluster units proceeds (after loss of the  $\mu_3\text{-S}^{2-}$  and the three terminal  $\text{S}_2^{2-}$  groups) by coalescence of the resulting unstable  $\text{Mo}_3\text{S}_6$  units [9b]. For  $\text{MoS}_3$  decomposition to  $\text{MoS}_2$ , Müller et al. also proposed a similar mechanism [28]. They argue that the decomposition product under moderate thermal treatments of both the trimer and  $\text{MoS}_3$  is  $\text{MoS}_2$ ; and also that much higher activation energies (of decomposition of  $\text{MoS}_3$ ) have to be expected with a different structural arrangement of the trisulphide, e.g., a chain-like one as proposed by Chien et al. [27].

We think that our results support the model of Müller et al. Thus, the break down of the  $\text{Mo}^{\text{V}}-\text{Mo}^{\text{V}}$  structure of the dimer [24] proceeds through  $\text{MoS}_3$  in order to attain a (necessary) short-order arrangement into triangular subunits. In agreement with Müller's arguments, a relatively high temperature ( $>400^\circ\text{C}$ ) is required for the decomposition of the dimer chain-like structure; also, a high activation energy was calculated for the reduction of this compound (Table 3). In contrast, in the case of the monomer, where no preformed Mo–Mo entities exist, production of  $\text{MoS}_3$  is much easier. The trimer, already possessing the required triangular subunits, does not decompose to  $\text{MoS}_3$  but directly to  $\text{MoS}_2$ . The activation energies obtained in these two cases are similar, again supporting the idea of a similar structural arrangement for both the trimer and  $\text{MoS}_3$ .

#### 4. Conclusions

The thermal decomposition of ammonium thiomolybdates in inert atmosphere results in the formation of stoichiometric  $\text{MoS}_2$  at temperatures higher than  $800^\circ\text{C}$ . The characteristics of each complex depend on its structure and the type of sulfur ligands present. For the monomer and dimer compounds,  $\text{MoS}_3$  was found to be an intermediate product. Hydrogen reduction does not affect the initial decomposition of the monomer and the dimer anions, but it does in the case of the trimer; hydrogen also accelerates the decomposition of  $\text{MoS}_3$ . In the presence of hydrogen,

stoichiometric MoS<sub>2</sub> is formed at temperatures lower than 450°C. Temperature-programmed reduction could be employed as a fingerprint technique for the identification of these compounds.

### Acknowledgements

It is a pleasure to acknowledge the support of CONICIT (Programa Nuevas Tecnologías) for part of the instrumentation employed in the present work (acquired through Grant QF-10). Thanks are also due to Micromeritics for the generous loan of the TPD/TPR 2900, and to Mary Labady and Beulah Griffe for their cooperation.

### References

- [1] (a) A. Müller, E. Diemann, R. Jostes and H. Bögge, *Angew. Chem. Int. Ed. Engl.*, 20 (1981) 934.  
(b) E.I. Stiefel, in H.F. Barry and P.C.H. Mitchell (Eds.), *Proceedings of the Fourth International Conference on the Chemistry and Uses of Molybdenum*, Climax Molybdenum Co., Ann Arbor, 1982, p. 56.
- [2] E. Diemann, Th. Weber and A. Müller, *J. Catal.*, 148 (1994) 288.
- [3] A. Müller, E. Diemann, A. Branding, F.W. Baumann, M. Breyse and M. Vrinat, *Appl. Catal.*, 62 (1990) L13.
- [4] S. Fuentes, G. Díaz, F. Pedraza, H. Rojas and N. Rosas, *J. Catal.*, 113 (1988) 535.
- [5] D.G. Kalthod and S.W. Weller, *J. Catal.*, 98 (1986) 572.
- [6] For example, R. Prins, V.H.J. De Beer and G.A. Somorjai, *Catal. Rev. Sci. Eng.*, 31 (1989) 1.
- [7] A.J. Jacobson, R.R. Chianelli, S.M. Rich and M.S. Whittingham, *Mater. Res. Bull.*, 14 (1979) 1437.
- [8] T.P. Prasad, E. Diemann and A. Müller, *J. Inorg. Nucl. Chem.*, 35 (1973) 1895.
- [9] (a) E. Diemann, A. Müller and P.J. Aymonino, *Z. Anorg. Allg. Chem.*, 479 (1981) 191.  
(b) A. Müller and E. Diemann, *Chimia*, 39 (1985) 312.
- [10] N.W. Hurst, S.J. Gentry, A. Jones and B.D. McNicol, *Catal. Rev. Sci. Eng.*, 24 (1982) 233.
- [11] S. Bhatia, J. Beltramini and D.D. Do, *Catal. Today*, 7 (1990) 309.
- [12] J.L. Brito, J. Laine and K.C. Pratt, *J. Mater. Sci.*, 24 (1989) 425.
- [13] C.I. Cabello, I.L. Botto and H.J. Thomas, *Thermochim. Acta*, 232 (1994) 183.
- [14] D.G. Kalthod and S.W. Weller, *J. Catal.*, 95 (1985) 455.
- [15] B. Müller, A.D. van Langeveld, J.A. Moulijn and H. Knözinger, *J. Phys. Chem.*, 97 (1993) 9028.
- [16] W.H. Pan, M.E. Leonowicz and E.I. Stiefel, *Inorg. Chem.*, 22 (1983) 672.
- [17] A. Müller and E. Krickemeyer, *Inorg. Synth.*, 27 (1990) 47.
- [18] Z.D. Chang and D.Z. Jian, *Thermochim. Acta*, 233 (1994) 87.
- [19] C.H. Chang and S.S. Chan, *J. Catal.*, 72 (1981) 139.
- [20] H.P. Klug and L.E. Alexander, *X-Ray Diffraction Procedures For Polycrystalline and Amorphous Materials*, John Wiley, New York, 2nd edn., 1974.
- [21] A. Müller, V. Wittneben, E. Krickemeyer, H. Bögge and M. Lemke, *Z. Anorg. Allg. Chem.*, 605 (1991) 175.
- [22] E. Ya. Rode and B.A. Lebedev, *Russ. J. Inorg. Chem.*, 6 (1961) 608.
- [23] A. Müller, W. Jaegermann and J.H. Enemark, *Coord. Chem. Rev.*, 46 (1982) 245.
- [24] A. Müller and E. Diemann, in G. Wilkinson, R.D. Gillard and J.A. McCleverty (Eds.), *Comprehensive Coordination Chemistry*, Pergamon, Oxford, 1988, Vol. 2, Chapter 16.1.
- [25] T. Ozawa, *J. Therm. Anal.*, 2 (1970) 301.
- [26] T. Komatsu and W.K. Hall, *J. Phys. Chem.*, 95 (1991) 9966.

- [27] F.Z. Chien, S.C. Moss, K.S. Liang and R.R. Chianelli, *Phys. Rev. B*, 29 (1984) 4606.
- [28] A. Müller, E. Diemann, E. Krickemeyer, H.-J. Walberg, H. Bögge and A. Armatage, *Eur. J. Solid State Inorg. Chem.*, 30 (1993) 565.
- [29] G.C. Stevens and T. Edmonds, *J. Catal.*, 37 (1975) 544.
- [30] E. Diemann, *Z. Anorg. Allg. Chem.*, 432 (1977) 127.